

# Supplementary information: Thickness optimization in wide range quasi omnidirectional 1-D photonic structures

Victor Castillo-Gallardo<sup>\*1,2,3</sup>, Luis Eduardo Puente-Díaz<sup>1,2,3</sup>, D. Ariza-Flores<sup>4</sup>, Hector Pérez-Aguilar<sup>3</sup>, W. Luis Mochán<sup>†2</sup>, and Vivechana Agarwal<sup>‡1</sup>

<sup>1</sup>Centro de Investigación en Ingeniería y Ciencias Aplicadas, Universidad del Estado de Morelos, Av. Universidad 1001 Col. Chamilpa, Cuernavaca, Morelos 62209, México.

<sup>2</sup>Instituto de Ciencias Físicas, Universidad Nacional Autónoma de México, Av. Universidad S/N, Col. Chamilpa, 62210 Cuernavaca, Morelos, México.

<sup>3</sup>Facultad de Ciencias Físico Matemáticas, Universidad Michoacana de San Nicolás de Hidalgo, Av. Francisco J. Múgica S/N 58030, Morelia, Mich., México.

<sup>4</sup>Conacyt-Universidad Autónoma de San Luis Potosí, Karakorum 1470, Lomas 4ta Secc, San Luis Potosí, S.L.P., 78210, México.

September 17, 2020

## 1 Development of the transfer matrix

If you consider that the system only varies on the  $z$  axis (as show in Fig. <sup>Fig1</sup> I(a)), the transfer matrix is  $M(z_2, z_1)$  a 2x2 matrix that relates the components of the electric field  $E_{\parallel}$  and the magnetic field  $H_{\parallel}$  parallel to the  $xy$  plane, and normal to the axis of the structure, evaluated at any two points  $z_2$  and  $z_1$

$$\begin{pmatrix} E_{\parallel} \\ H_{\parallel} \end{pmatrix}_{z_2} = M(z_2, z_1) \begin{pmatrix} E_{\parallel} \\ H_{\parallel} \end{pmatrix}_{z_1}.$$

Many equivalent formulations have been proposed to obtain  $M$ . For example, if you have a complete multilayer system and it periodically replicates to form an artificial photonic crystal, then Bloch's theorem can be used to describe the normal modes of this crystal. According to Bloch's theorem, the modes of a periodic system may be written as a superposition of Bloch waves, each of which

---

\*email: victor1.1@hotmail.com

†email: mochan@fis.unam.mx

‡email: vagarwal@uaem.mx

acquires a *phase factor* as it propagates from one period to the next. Therefore, each Bloch wave would obey

$$\begin{pmatrix} E_{\parallel}^{\pm} \\ H_{\parallel}^{\pm} \end{pmatrix}_{z_N} = M \begin{pmatrix} E_{\parallel}^{\pm} \\ H_{\parallel}^{\pm} \end{pmatrix}_{z_0} = e^{\pm iKD} \begin{pmatrix} E_{\parallel}^{\pm} \\ H_{\parallel}^{\pm} \end{pmatrix}_{z_0}, \quad (1) \quad \boxed{\text{Bloch}}$$

where  $D = z_N - z_0$  is the period, which corresponds to the actual thickness of the multilayered system, and  $\pm K$  represents a 1D Bloch's vector corresponding to a wave that propagates along  $z$ -direction. Thus,  $\Lambda_{\pm} = e^{\pm iKD}$  are the eigenvalues of transfer matrix  $M$  and  $E_{\parallel}^{\pm}$  and  $H_{\parallel}^{\pm}$  are the corresponding eigenvectors. Notice that exactly  $\det M = 1$  is used, so that the product of eigenvalues ought to be  $\Lambda_+ \Lambda_- = 1$ , and the dispersion relation of the Bloch modes may be obtained in principle from

$$\cos KD = \frac{1}{2} \text{Tr } M \quad (2) \quad \boxed{\text{dispersion}}$$

where  $\text{Tr}$  denotes the trace.

Now, considering a finite system made of  $P$  periods, with  $PD$  thickness and placed on a substrate. For the extreme case of only  $P = 1$  period, the optical properties of this system can be obtained by considering an incoming wave from the ambient, a wave reflected to the environment, a wave transmitted to the substrate, and two Bloch waves within the structure, one moving up and other down, as show in Fig. 1(b).

Hence, the continuity of  $E_{\parallel}$  and  $H_{\parallel}$  will produce two equations at each interface, with which the four unknowns are obtained, namely  $r$ ,  $t$  and the amplitudes of two Bloch's waves. In a finite system,  $K$  can be complex. Even in the presence of very little dissipation, Bloch's waves should decay as they propagate. Thus, the eigenvalue of ascending mode  $\Lambda_+ = e^{iKD}$  is identified as the one that obeys  $|\Lambda_+| < 1$ ,  $\text{Im}K > 0$ , adding a negligible amount of dissipation if necessary to avoid cases  $|\Lambda_+| = 1$ .

From the eigenvalues  $\Lambda_{\pm}$  of the transfer matrix, we may obtain the corresponding eigenvectors  $E_{\parallel}^{\pm}$  and  $H_{\parallel}^{\pm}$  from Eq. (1), and from them, the corresponding surfaces impedances

$$Z^{\pm} = -\frac{M_{12}}{M_{11} - \Lambda_{\pm}}, \quad (3) \quad \boxed{Z^{\pm}}$$

where  $M_{ij}$  with  $i = 1, 2$  and  $j = 1, 2$  denote the elements of the transfer matrix  $M$ . By writing the fields at  $z_0$  and  $z_N$  as a superposition of the upward and downward propagating (or decaying) fields,  $E_{\parallel}^{\pm} = Z^{\pm} H_{\parallel}^{\pm}$ , we can relate the fields at  $z_N$  to the fields at  $z_0$  through a *reconstructed* transfer matrix,

$$\begin{pmatrix} E_{\parallel} \\ H_{\parallel} \end{pmatrix}_{z_N} = \tilde{M} \begin{pmatrix} E_{\parallel} \\ H_{\parallel} \end{pmatrix}_{z_0}, \quad (4) \quad \boxed{\text{tilMEH}}$$

where

$$\tilde{M} = \frac{1}{Z^+ - Z^-} \begin{pmatrix} Z^+ e^{iKD} - Z^- e^{-iKD} & -2iZ^+ Z^- \sin KD \\ 2i \sin KD & Z^+ e^{-iKD} - Z^- e^{iKD} \end{pmatrix}. \quad (5) \quad \boxed{\text{tilM}}$$

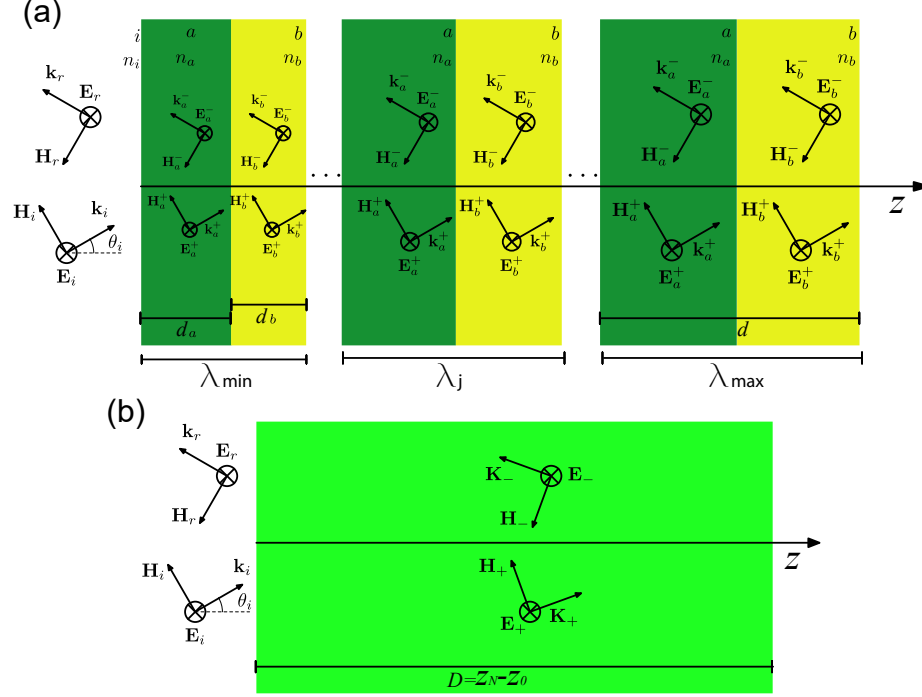


Figure 1: (a) Chirped-type photonic structure formed by two alternating materials  $a$  and  $b$ , with refractive indices  $n_a$  and  $n_b$ , and their thickness  $d_a$  and  $d_b$  gradually increases according to the condition of  $1/4$  of the wavelength at which  $j$ -th. period will be sintonized.  $\mathbf{E}_\alpha^\beta$  and  $\mathbf{H}_\alpha^\beta$  are the electric and magnetic fields, and  $\mathbf{k}_\alpha^\beta$  is the wavevector, where  $\alpha = \{i, r, a, b\}$  corresponds to the medium where the wave is traveling and  $\beta = \{-, +\}$  to the direction of propagation of the wave along the  $\pm z$  axis. (b) The multilayer system can be replaced by a broad effective layer within which the electric  $\mathbf{E}_\beta$  and magnetic  $\mathbf{H}_\beta$  fields, and a Bloch wave  $\mathbf{K}_\beta$  propagate in the positive direction and another set propagate in the opposite direction along the  $z$  axis.

Fig1

Finally, the explicit expressions for the optical coefficients are:

$$r = \mp \frac{Z_0 \tilde{M}_{11} + \tilde{M}_{12} - Z_0 Z_s \tilde{M}_{21} - Z_s \tilde{M}_{22}}{Z_0 \tilde{M}_{11} - \tilde{M}_{12} - Z_0 Z_s \tilde{M}_{21} + Z_s \tilde{M}_{22}}, \quad (6) \quad \boxed{\text{rBloch}}$$

and

$$t = \frac{2Z_\alpha}{Z_0 \tilde{M}_{11} - \tilde{M}_{12} - Z_0 Z_s \tilde{M}_{21} + Z_s \tilde{M}_{22}}, \quad (7) \quad \boxed{\text{tBloch}}$$

where the upper sign  $-$  in Eq. (6)<sup>rBloch</sup> and the subscript  $\alpha = s$  in Eq. (7)<sup>tBloch</sup> has been chosen for the case of TE polarization, while the lower sign  $+$  and the subscript  $\alpha = 0$  correspond to TM polarization. As usual, the reflectance is given by  $R = |r|^2$  and the transmittance by  $T = \beta |t|^2$  with  $\beta = Z_0/Z_s$  for the case of TE polarization and  $\beta = Z_s/Z_0$  for the case of TM polarization.

## 2 Chirped-type Bragg mirrors

As the porosity contrast of the periods increases, the thickness of the structure decreases and the average reflectance increases, as shown in table 1. For example, you could have structures with a thickness of 10  $\mu\text{m}$  and their average reflectance greater than 90%.

Table 1: Design parameters obtained after the optimization of functions for maximum average reflectance and minimum thickness

Function	Porosity		$\lambda_0$ ( $\mu\text{m}$ )		$\alpha$	$\beta$	$A$	Periods	Thickness ( $\mu\text{m}$ )	$R_{\text{ave}}$ %
	Low	High	Min	Max						
$f_1$	30	76	0.40	1.4	0.55	----	----	30	9.2	92
$f_i$	42	76	0.40	1.4	0.35	----	----	101	35.7	91
$f_2$	30	76	0.43	1.4	0.22	4.30	0.49	66	17.8	93
$f_2$	42	76	0.41	1.4	0.45	1.23	0.51	30	8.9	89
$f_3$	30	76	0.40	1.4	1.15	0.56	0.09	30	10.5	91
$f_3$	42	76	0.35	1.4	1.01	0.50	0.10	50	16.4	90

The mapping of the calculated reflectance of the structures designed with the optimized parameters is shown in Fig. 2.<sup>Fig2</sup> Here it is observed that all of them have a PBG in the NIR region of the electromagnetic spectrum, i. e., structures designed from functions  $f_1$  and  $f_3$  with a porosity contrast of 30/76% have the highest PBG localized from 970 to 1370 nm, these are shown in panels (a) and (c).

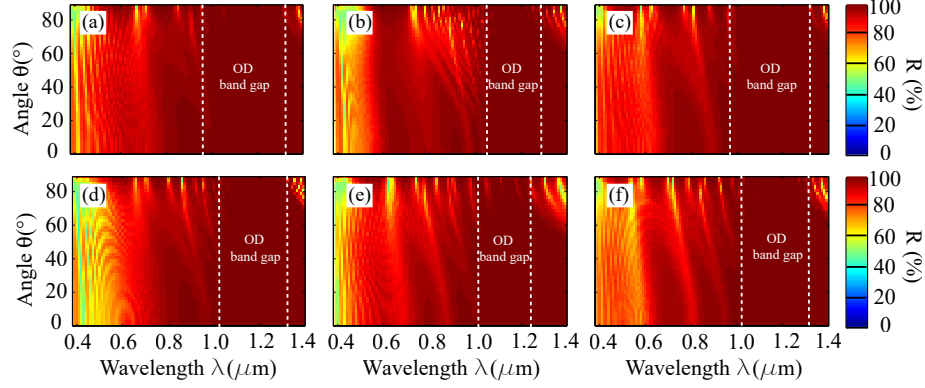


Figure 2: Calculated reflectance of the structures designed with the optimized parameters of  $f_1$  (left),  $f_2$  (center) and  $f_3$  (right) and with the porosity contrasts of 30/76% (upper panels) and 42/76% (lower panels). The dotted lines limit the area of the PBG.

Fig2

### 3 Photonic structure with sub-mirrors stacking

Before showing the design of the structures formed by the stacking of sub-mirrors, the transfer matrix trace of individual mirrors formed by one period (Fig. 3(a)) and six periods (Fig. 3(b)) was calculated. The reflectance of each mirror with its respective periods was also calculated (Figs. 3(c) and 3(d)). Each mirror was designed to reflect a wavelength in the range of 400-3000 nm and the illumination range was the same. Additionally, the  $Tr|M|$  and  $R(\lambda, \theta)$  were calculated for light with TE polarization and  $45^\circ$  of incidence. In Fig. 3d it is shown that by using mirrors that have 6 periods and designed to reflect at wavelengths greater than 1000 nm, they also reflect in a certain region of the visible spectrum. Then, to reinforce the reflection of the electromagnetic waves in the visible, it is enough to place a smaller number of periods. This is another reason for the increasing number of periods in the 400 to 800 nm region.

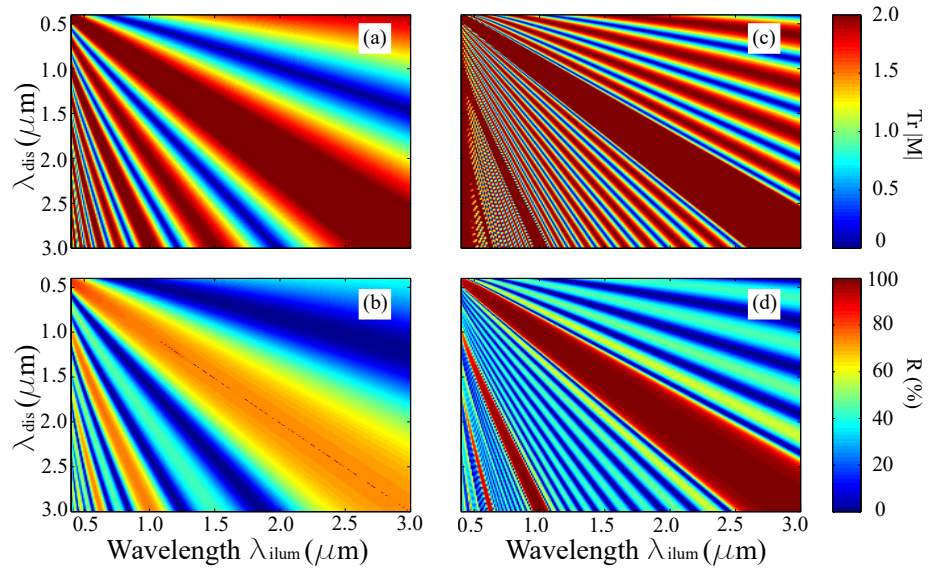


Figure 3: Calculated transfer matrix trace and reflectance of individual mirrors using ((a) and (c)) one period and ((b) and (d)) six periods, respectively. Each mirror was tuned to a wavelength between 400 and 3000 nm. The calculations were made in the visible and NIR region and at  $45^\circ$  of incidence.

**Fig3**

It is common to imagine that the stacking of the sub-mirrors is the following: that the PBG of the second mirror begins at the edge of the PBG of the first mirror, the third PBG that begins at the edge of the PBG of the second mirror, and so on until the desired interval is completed. With this configuration, the reflectance decreases at each intersection of the two PBGs. For example, in Figs. 4(a) and 4(b) show the calculated  $R(\lambda, \theta)$  for the structures formed by sub-mirrors that have one and six periods, respectively, using non-polarized light. In these cases, the calculations do not show a PBG, or quasi-PBG. For this reason, the  $R_{Ave}(\lambda, \theta)$  was maximized through the percentage of overlap of the PBGs of two consecutive sub-mirrors. In Fig. 3 (b) of the main article the results obtained at the end of the optimization process are shown. The calculated  $R(\lambda, \theta)$  for the structures designed with 4 periods for each sub-mirror and using the pattern described in the main article are shown in Figs. 4(c) and 4(d) of this document, respectively. Here the overlap of the two consecutive PBGs was optimized, being 72% for the first case and 78% for the last. Furthermore, the calculations indicate that the structures have a quasi-PBG.

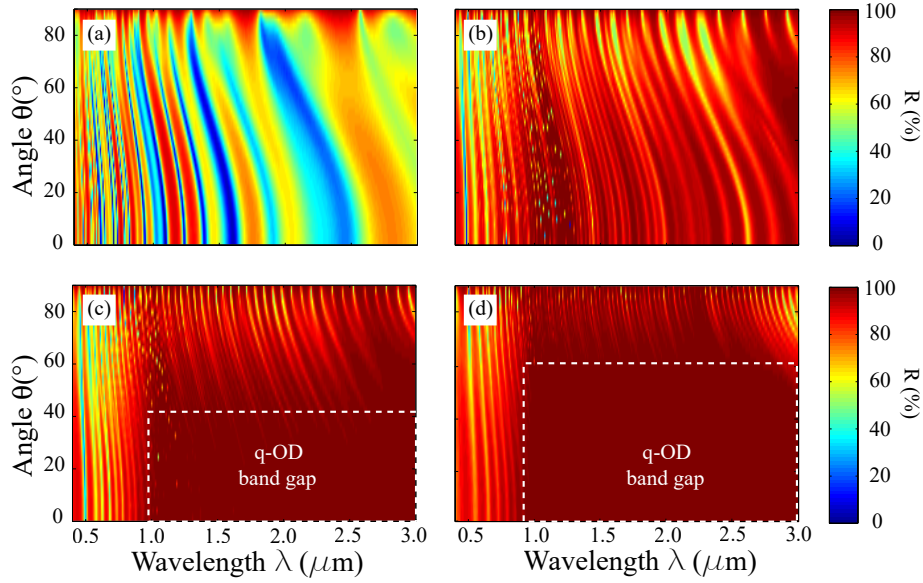


Figure 4: Reflectance calculated for structures designed through the stacking of sub-mirrors analyzing the overlap of the PBG and the number of periods of each one of them. Case I: there is no overlap of the PBGs and each sub-mirror has (a) one period and (b) six periods. Case II: optimized overlap of consecutive PBGs and (c) each subsmirror has 4 periods with 72% overlap, and (d) proposed arrangement in the main article with 6 periods for  $\lambda > 800$  nm and 78% overlap. The quasi-OD region is bounded by the dotted lines.

Fig4